Liquefaction-Induced Settlement Estimates for a Spatially Variable Deposit Using Numerical and Empirical Approaches

Devdeep Basu[1], Jack Montgomery[2], and Armin W. Stuedlein[3]

[1]Department of Civil Engineering, Auburn University, Auburn, Alabama, USA.
E-mail: dzb0048@auburn.edu
[2]Department of Civil Engineering, Auburn University, Auburn, Alabama, USA.
E-mail: jmontgomery@auburn.edu
[3]Department of Civil Engineering, Oregon State University, Corvallis, Oregon, USA.
E-mail: armin.stuedlein@oregonstate.edu

Abstract: Liquefaction of soil during earthquakes poses a major threat to both aboveground and buried infrastructure. Designing effective mitigation strategies for liquefaction requires tools, which can accurately predict associated deformations. Several empirical models have previously been developed to predict the post-liquefaction reconsolidation settlements as well as potential for differential settlements. However, most of these models assume one-dimensional strains, which is equivalent to assuming the soil is laterally homogeneous. These models cannot directly account for the effects of spatial variability in a soil deposit. Numerical models on the other hand can incorporate this spatial variability to estimate liquefaction-induced deformations. This study focusses on liquefaction assessment using 1D and 2D numerical models developed for a test site located near Hollywood, South Carolina in USA. These models incorporate the spatial variability of the soil estimated at the site through previous studies. The liquefaction-induced settlements are correlated with the shear strain patterns observed at the end of earthquake shaking, leading to differences between the 1D and 2D modeling approaches. The numerical responses are also compared with results from an empirical model. The findings show that the 1D numerical models tend to over-predict and the 2D numerical models tend to under-predict differential settlements compared with the empirical model for this site and the selected ground motion. Additional work is needed to determine if these patterns hold for other conditions.

Keywords: Liquefaction; spatial variability; numerical modeling; differential settlement.

1 Introduction

Cyclic loading from earthquakes can generate considerable excess pore pressures and shear strains in granular soils leading to liquefaction. After shaking, the excess pore pressures start dissipating and the outflow of water leads to reconsolidation of the soil and settlement of the ground surface. These settlements can cause significant damage to overlying infrastructure (e.g., buildings and bridges) as well as to underground structures (e.g., buried utilities), especially if considerable differential settlement occurs. Several empirical models to predict post-liquefaction settlements using laboratory experiments and field observations have been developed over the years (Tokimatsu and Seed 1987; Ishihara and Yoshimine 1992; Sento et al. 2004; Yoshimine et al. 2006; Idriss and Boulanger 2008). These models commonly estimate potential post-liquefaction volumetric strains using profiles of penetration resistances from standard penetration tests (SPTs) or cone penetration test (CPTs) and estimates of earthquake loading. These volumetric strains can then be used to estimate settlements. Owing to their one-dimensional (1D) formulation, the empirical models necessarily treat the soil as laterally homogeneous. The effects of spatial variability in soil properties can be taken into account by using numerical models (e.g., Popescu et al. 1997; Montgomery and Boulanger 2017), but these models are not commonly used in practice.

In this paper, numerical simulations are performed for a test site at Hollywood, South Carolina, USA. The test site had been well characterized previously through a number of CPT tests, downhole shear wave velocity tests and mud rotary borings (Stuedlein et al. 2016; Gianella and Stuedlein 2017). Bong and Stuedlein (2018) examined the spatial variability of the site and developed a three-dimensional (3D) geostatistical model for the site. This study will simulate cross-sections from this geostatistical model using the finite difference program FLAC (v7.0; Itasca 2014). Both 2D (using an entire cross-section) and 1D (considering each column of elements of a cross-section individually) numerical simulations are performed for two cross-sections from the 3D geostatistical model. The results of the numerical simulations are compared with results from an empirical model (Yoshimine et al. 2006; Idriss and Boulanger 2008). The results show that the predicted differential settlements from the numerical simulations can be correlated with the pattern of shear strains within the soil at the end of shaking. The numerical models predict deformations will concentrate in narrow bands, while the empirical model predicts uniform strains throughout the layer leading to differences in settlement patterns.

2 Liquefaction Test Site – Hollywood, SC

Proceedings of the 7th International Symposium on Geotechnical Safety and Risk (ISGSR)
Editors: Jianye Ching, Dian-Qing Li and Jie Zhang

Published by Research Publishing, Singapore.
ISBN: 978-981-11-2725-0; doi:10.3850/978-981-11-2725-0_IS5-7-cd

This study focuses on a liquefaction test site in Hollywood, South Carolina, USA. A number of geotechnical studies have been performed at this site, including evaluation of liquefaction mitigation using driven displacement piles (Stuedlein et al. 2016) and controlled blasting (Gianella and Stuedlein 2017), as well as effects of pile spacing and installation on driving and penetration resistance (Stuedlein and Gianella 2016). The site has also been extensively characterized using CPT soundings, downhole- and surface wave-based shear wave velocity tests, and mud-rotary borings with split-spoon samples. The spatial variability of the liquefiable soil layer and effects of this variability on liquefaction-induced settlement has been extensively studied (Bong and Studlein 2017; Bong and Studlein 2018). Figure 1 shows a plan view of the test site in Hollywood, SC along with the various geotechnical test locations at the site.

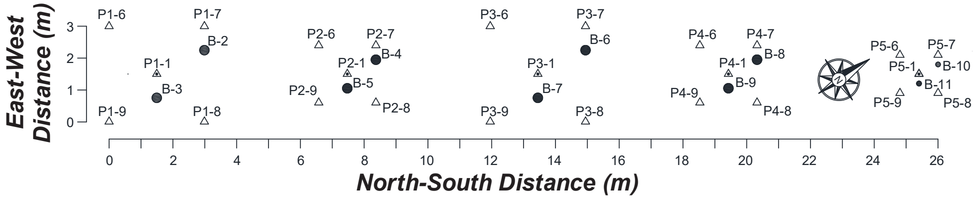

Figure 1. Plan view of the Hollywood test site showing exploration locations (modified from Bong and Stuedlein 2018).

The general stratigraphy at the Hollywood site comprises an 8.5 m thick potentially liquefiable layer of loose to medium dense poorly graded sand with lenses of silty sand, overlain by a 2.5 m loose to medium dense silty or clayey sand fill layer. The liquefiable layer is underlain by a 1.5 m soft to medium stiff clay layer, which is underlain by a dense sand layer. The thicknesses of the layers are relatively uniform across the site and the water table depth, which exhibits seasonal variation, could be as shallow as 2 m. Figure 2 shows the general stratigraphy at the site along with the measured CPT data with depth at two locations in the site.

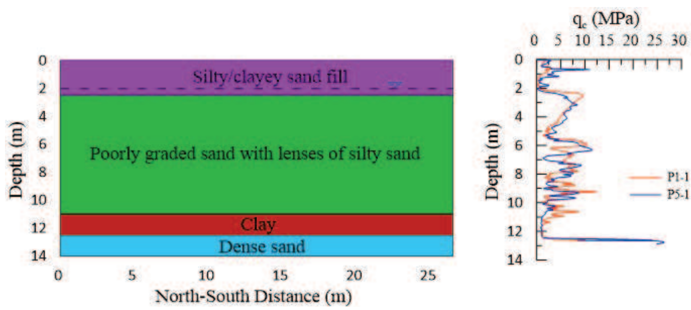

Figure 2. General site stratigraphy at Hollywood test site and measured CPT profile at two locations.

Bong and Stuedlein (2017) developed a three-dimensional (3D) geostatistical model of corrected cone-tip resistance (q_{c1Ncs}) and fines content within the liquefiable layer using random field modeling. The geostatistical model was discretized at intervals of approximately 25 cm in the horizontal directions (from 0 m to 3 m in the E-W direction and 0 m to 26 m in the N-S direction) and at intervals of 2 cm vertically with depth (from 2.5 m to 11 m). Basu et al. (2019) used this geostatistical model to numerically examine settlement patterns at the site. In order to reduce the computational effort required for the simulations they developed 2D cross-sections from the geostatistical model by averaging the CPT data from the original geostatistical fields in order to obtain a 2D model with element dimensions of 50 cm both in the vertical and north-south directions. This resulted in a total of 13 cross-sections in the east-west directions (at intervals of 25 cm). The averaged fines corrected cone-tip resistance (q_{c1Ncs}) for the two 2D cross-sections are shown in Figure 3. Basu et al. (2019) examined all 13 cross-sections using 2D numerical simulations and empirical models and a suite of ground motions for a strike-slip event with a moment magnitude (M_w) of 7 at distance of 10 km. Basu et al. (2019) found that numerical simulations tended to underestimate settlements in comparison with the empirical models. They also found that the numerical simulations tended to predict less differential settlement across the site than would be expected from the empirical model. They attributed this difference primarily to pore pressure diffusion between looser and denser zones that resulted in a more uniform distribution of pore pressure than would be predicted with a 1D model. This study expands on this previous work by using 1D numerical simulations in addition to the 2D models. The results are again compared with the settlements predicted from empirical approaches.

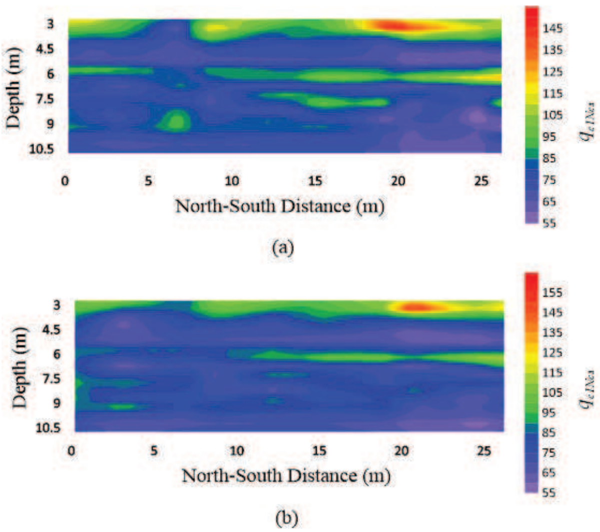

Figure 3. Contours of q_{c1Ncs} at Hollywood test site for two cross-sections at: (a) 0.25 m (b) 2.25 m in the E-W direction.

3 Empirical Model

The empirical approach outlined by Ishihara and Yoshimine (1992) and Yoshimine et al. (2006) was used to estimate the maximum shear strain and the reconsolidation settlement for the two cross-sections. This approach utilizes the CPT tip resistance, factor of safety against liquefaction, and maximum shear strains to estimate the volumetric strains at each depth within a soil profile. These strains can then be multiplied by the layer thicknesses to estimate the total settlement of the profile (0.5 meters in this study). For this study, the factor of safety against liquefaction was evaluated from the CPT based liquefaction triggering framework by Idriss and Boulanger (2008).

4 Numerical Model

In this present study, 1D and 2D numerical models for two soil cross-sections at Hollywood test site were analyzed using the finite difference program FLAC (v7.0; Itasca 2014). Square elements having a size of 50 cm were used for the models. The 2D simulations considered cross-sections having a width of 26 m and running along the north-south direction (Figure 2). The 1D models were created by simulating each column within the 2D model individually. The models had a total depth of 14 m and the water table depth was taken at 2 m below the ground surface. The analysis were performed in three stages. In the first stage, the model was brought to static equilibrium with the base of the model fixed and allowing for vertical displacement along the sides only. No flow was allowed from either the base or the sides of the model. In the second stage, an earthquake shaking was applied at the base of the model as a horizontal acceleration-time history with the base fixed against vertical movement and periodic boundary conditions on the sides of the model. The Mudurnu recording from the 1999 Duzce, Turkey earthquake was used for this study. The record was linearly scaled to achieve a PGA of 0.15g (Figure 4). This earthquake recording was selected because it produced approximately median settlements among the suite of motions used by Basu et al. (2019) to examine the Hollywood site. In the third stage, the model was allowed to reconsolidate with the same boundary conditions as in the first stage.

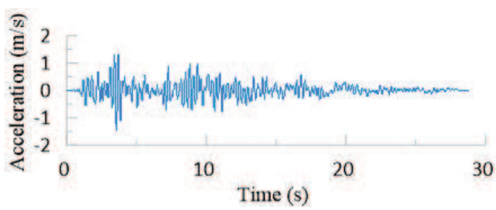

Figure 4. Acceleration time history of the Duzce, Turkey earthquake record of 1999 linearly scaled up to 0.15g PGA.

The dense sand, liquefiable sand, and fill layers were modeled using PM4Sand (Boulanger and Ziotopoulou 2015), a bounding surface plasticity model which has the ability to model the cyclic behavior of sands during both the cyclic mobility and reconsolidation phases of liquefaction. This model has been successfully used to simulate the effects of spatial variability on liquefaction-induced deformations for sloping ground (Montgomery and Boulanger 2017) and earth dams (Boulanger and Montgomery 2016) in the past. The three major input parameters for PM4Sand are the apparent relative density (D_r) as estimated from the q_{c1Ncs} (Idriss and Boulanger 2008), the shear modulus coefficient (G_o) as calculated from the stress normalized shear wave velocity (V_{s1}) of the soil, and contraction rate parameter (h_{po}), which is calibrated using single element direct simple shear simulations to obtain the desired cyclic strength. For this study, the desired cyclic resistance ratio was estimated using the CPT based triggering relationship proposed by Idriss and Boulanger (2008) with a reduction of 10% and an upper limit on the cyclic stress ratio of 0.8 for very dense soils. The reduction of 10% in the cyclic strength was used to provide better agreement in terms of the extent of liquefaction between the numerical simulations and the empirical approaches. This reduction led to better agreement with the empirical settlement results than obtained by Basu et al. (2019) who used the unmodified triggering curve. The parameters controlling the reconsolidation phase were recalibrated by Basu et al. (2019) to achieve a better match between the numerical and the empirical settlement estimates for uniform models and these recalibrated parameters have been adopted for this study. All other model parameters retained their default values (Boulanger and Ziotopoulou 2015).

The properties of the liquefiable layer were correlated to the random fields of q_{c1Ncs} (Figure 3). The V_{s1} was correlated to the q_{c1Ncs} (Equation 1) by modifying the default correlation between G_o and D_r (Boulanger and Ziotopoulou 2015) to obtain a better match with the measured average V_{s1} at the Hollywood site (Mahvelati et al. 2016). The calibration of h_{po} was done for 34 values of q_{c1Ncs} ranging from 21 to 254, which covers the total range of values in the random fields and linear interpolation was used to determine h_{po} for intermediate values of q_{c1Ncs}. The permeability of each element of the liquefiable layer was determined using the geostatistical model of fines content developed by Bong and Stuedlein (2017) and a modified form of the correlation proposed by Rawls and Brakensiek (1985). The permeability values obtained from the original Rawls and Brakensiek (1985) equation were scaled down by two orders of magnitude to better match the average permeability measured at the site (Stuedlein and Gianella 2016).

$$V_{s1} = 45.5\left(q_{c1Ncs}\right)^{0.3244} \tag{1}$$

The other non-liquefiable layers were assigned uniform properties in order to isolate the effects of spatial variability in the liquefiable layer. Table 1 outlines some of these properties for the uniform layers. The properties for these layers were taken from Stuedlein and Gianella (2016) or assumed based on the soil type. The clay layer was modeled using an elastic-plastic Mohr-Coulomb constitutive model with an undrained shear strength and a friction angle of zero. The shear wave velocity of the layer was 168 m/s. The fill and dense sand layers were modeled with PM4Sand and were assigned uniform relative densities of 80% and 90%, respectively, based on the CPT data. The correlations of Boulanger and Ziotopoulou (2015) were used to estimate G_o. The permeabilities for the fill and dense sand layers were assumed to be equal to the average value for the liquefiable layer and the permeability of the clay layer was assumed to be two orders of magnitude lower than the sands.

Table 1. Soil properties selected for the non-liquefiable layers in the numerical model.

Layer	Input properties						
	Cohesion (kPa)	Friction angle (deg)	Dry density (kg/m^3)	D_r	q_{c1Ncs}	Maximum shear modulus (kPa)	Permeability (cm/s)
Fill	-	-	1712	0.8	174	1.1x10^5	0.01
Clay	38	0	1800	-	-	5x10^4	0.0001
Dense sand	-	-	1745	0.9	211	1.2x10^5	0.01

5 Results

Both 1D and 2D simulations were performed using a PGA of 0.15g (Figure 4). Figures 5 and 6 show the maximum shear strain variation across the liquefiable layer for both the 1D and 2D numerical models (section 0.25 m in E-W direction), respectively, and the corresponding surface settlements. The maximum shear strain corresponds to the largest value at any time during the earthquake shaking. The 1D simulations are individually performed for each column and then the values from each simulation are contoured together in Figure 4. The 1D and 2D simulations show similar patterns of shear strain, with deformations concentrating in two bands. The magnitude of strains within each band shows more variation in the 1D simulations, as each column is evaluated independently. In the 2D model, the strain values tend to be similar between adjacent elements leading to a more uniform distribution of strain. Similarly, the settlement profiles observed from the two models show more differential settlement for the 1D model, whereas the 2D model shows a more uniform settlement. However, the average settlement value is similar for both models. The simulations were repeated using the other cross-section (2.25 m in E-W direction) and similar patterns of both shear strain and settlement were observed.

The empirical model was also used to estimate settlements for a PGA of 0.15g and a M_w=7 earthquake. The empirical model predicted larger average settlements than the numerical models (Figures 5 and 6), but the agreement is better than was observed by Basu et al. (2019) due to the reduction in cyclic strength used in this study. The settlement at either edges of the profile is observed to have a slight dip. This is due to a slightly higher average q_{c1Ncs} in the columns on either edge, which decreases the volumetric strains and therefore decreases the settlement. The empirical model predicted uniform shear strains of approximately 8% across the entire liquefiable layer, which led to relatively low estimates of differential settlement. These differential settlement estimates are lower than those found by Bong and Stuedlein (2018) due to the averaging used in this study. The maximum differential settlement predicted by the empirical model was 5 cm while the 1D model predicted differential settlements of 11 cm. The 2D numerical model predicted maximum differential settlements of only 2 cm.

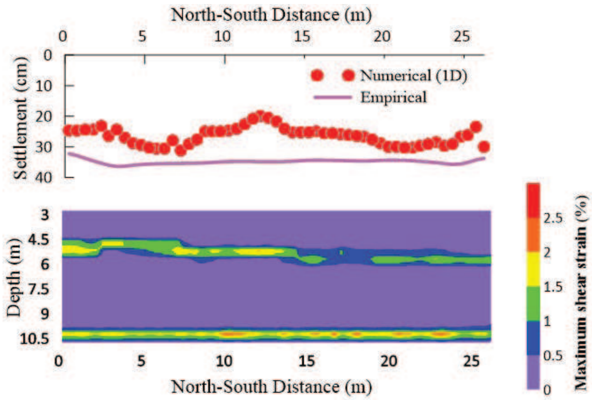

Figure 5. Maximum shear strain variation (1D model) in the liquefiable layer for cross-section at 0.25 m in E-W direction.

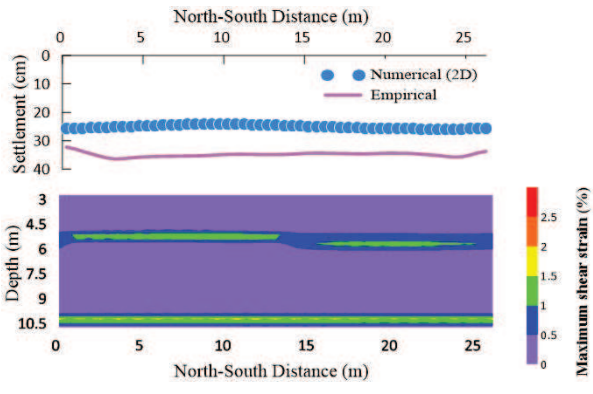

Figure 6. Maximum shear strain variation (2D model) in the liquefiable layer for cross-section at 0.25 m in E-W direction.

Differences in estimates of differential settlement between the three models are attributed to two main sources. The first is differences in the distribution of shear strains in the model, which are directly correlated to post-shaking volumetric strains (Ishihara and Yoshimine 1992). In the numerical models, shear strains tended to concentrate in two bands. The empirical model evaluates each depth independently and so cannot account for these types of strain concentrations. This led to uniform strain estimates for the entire depth. The 1D numerical simulations showed a discontinuous pattern of shear strains which led to differences in volumetric strains and therefore settlement. In the 2D simulation, the columns were forced to move together leading to an averaging of the response across the model. This lead to similar magnitudes of volumetric strains post-shaking. The second factor was diffusion of excess pore pressures between loose and dense zones in the 2D model. This tends to further average settlements leading to reduced differential settlements. The 1D and empirical models cannot directly account for effects of pore pressure diffusion and therefore predict larger differential settlements.

6 Discussion and Conclusions

This study performed 1D and 2D numerical simulations to estimate patterns of liquefaction-induced settlements for two cross-sections at a well-characterized test site in Hollywood, South Carolina, USA. The PM4Sand constitutive model (Boulanger and Ziotopoulou 2015) was used to model the liquefiable sand layer. Spatial variability in the properties of the sand layer was represented using random fields and simulations were performed for both 1D columns and a 2D section. The results from the numerical simulations were compared with an empirical model (Yoshimine et al. 2006) for estimating reconsolidation settlements. The average magnitude of settlement was similar between the three approaches, but significant differences in the magnitude of differential settlement were observed.

The numerical simulations showed that shear strains tended to concentrate in two narrow bands for both the 1D and 2D models. The 2D models showed more uniform magnitudes of shear strain across the bands than were observed in the 1D columns. This difference could be attributed to averaging which occurs in case of 2D models as the strains of one column are tied together with those of adjacent columns. The empirical model predicted uniform strains across the layer and therefore showed less differential settlement than the 1D numerical simulations. The empirical model did predict more differential settlement than the 2D numerical simulations, which is primarily attributed to diffusion of excess pore pressures between looser and denser zones in the numerical simulations. This leads to more uniform distributions of excess pore pressure and therefore reconsolidation settlements. Additional work is need to examine the effects of ground motion variability and constitutive model calibration on the results. It would also be beneficial to examine these effects for sites with different levels of spatial variability to determine if similar patterns are observed.

References

Bong, T. and Stuedlein, A.W. (2017). Spatial variability of CPT parameters and silty fines in liquefiable beach sands. *Journal of Geotechnical and Geoenvironmental Engineering*, 143(12), 1-13.

Bong, T. and Stuedlein, A.W. (2018). Effect of Cone Penetration Conditioning on Random Field Model Parameters and Impact of Spatial Variability on Liquefaction-induced Differential Settlements. *Journal of Geotechnical and Geoenvironmental Engineering*, 144(5), 1-14.

Basu, D., Montgomery, J., and Stuedlein, A.W. (2019). Estimation of reconsolidation settlements due to liquefaction using numerical and empirical models. *7th ICEGE* (Accepted).

Boulanger, R.W., and Idriss, I.M. (2015). CPT-based liquefaction triggering procedures. *Journal of Geotechnical and Geoenvironmental Engineering*, 142(2), 1-11.

Boulanger, R.W. and Montgomery, J. (2016). Nonlinear deformation analyses of an embankment dam on a spatially variable liquefiable deposit. *Soil Dynamics and Earthquake Engineering*, 91, 222-233.

Boulanger, R.W. and Ziotopoulou, K. (2015). PM4Sand (version 3): A sand plasticity model for earthquake engineering applications. *Rep No. UCD/CGM-15/01,* Center for Geotechnical Modeling, Department of Civil and Environmental Engineering, University of California, Davis, CA.

Gianella, T.N. and Stuedlein, A.W. (2017). Performance of driven displacement pile-improved ground in controlled blasting field tests. *Journal of Geotechnical and Geoenvironmental Engineering*, 143(9), 04017047.

Idriss, I.M. and Boulanger, R.W. (2008). Soil liquefaction during earthquakes. *Monograph MNO-12,* Earthquake Eng. Research Institute, Oakland, CA.

Ishihara, K. and Yoshimine, M. (1992). Evaluation of settlements in sand deposits following liquefaction during earthquakes. *Soils and Foundations*, 32(1), 173-188.

Itasca. (2014). FLAC. *Fast Lagrangian analysis of continua, user's guide, version 7.0*, Minneapolis.

Mahvelati, S., Coe, J.T., Stuedlein, A.W., Asabere, P., and Ginaella T.N. (2016). Time-rate variation of the shear wave velocity following blast induced liquefaction. *Geo-Chicago GSP 271*, 904-913.

Montgomery, J. and Boulanger, R.W. (2017). Effects of spatial variability on liquefaction-induced settlement and lateral spreading. *Journal of Geotechnical and Geoenvironmental Engineering*, 143(1), 1-15.

Popescu, R., Prevost, J.H., and Deodatis, G. (1997). Effects of spatial variability on soil liquefaction: Some design recommendations. *Geotechnique*, 47(5), 1019-1036.

Rawls, W.J. and Brakensiek, D.L. (1985). Prediction of soil water properties for hydrologic modelling. In E.B. Jones & T.J. Ward (eds), *Proceedings, Symposium of Watershed Management in the Eighties*, 293-299, New York.

Sento, N., Kazama, M., Uzuoka, R., Ohmura, H., and Ishimaru, M. (2004). Possibility of post-liquefaction flow failure due to seepage. *Journal of Geotechnical and Geoenvironmental Engineering*, 13(7), 707-716.

Stuedlein, A.W. and Gianella, T. (2016). Drained timber pile ground improvement for liquefaction mitigation. *NCHRP IDEA project report 180,* Transportation Research Board.

Tokimatsu, K. and Seed, H.B. (1987). Evaluation of settlements in sand due to earthquake shaking. *Journal of Geotechnical Engineering*, ASCE, 113(8), 861-878.

Yoshimine, M., Nishizaki, H., Amano, K., and Hosono, Y. (2006). Flow deformation of liquefied sand under constant shear load and its application to analysis of flow slide in infinite slope. *Soil Dynamics and Earthquake Engineering*, 26, 253-264.